

Gas-Phase Negative Ion Chemistry of Lewis Acid–Base Complexes

Jianhua Ren, Derek B. Workman, and Robert R. Squires*

Contribution from the Department of Chemistry, Purdue University, West Lafayette, Indiana 47907

Received February 9, 1998

Abstract: The gas-phase negative ion chemistry of a series of Lewis acid–base complexes [Me_2SBH_3 (**1**), Me_3NBH_3 (**2**), Me_3PBH_3 (**3**), Me_2SBF_3 (**4**), Me_2OBF_3 , Et_3NBH_3 , and Et_2OBF_3] was investigated with use of the flowing afterglow triple-quadrupole technique. Ab initio MO calculations using the G2(MP2) and CBS-4 models were carried out for **1–4** and related species. The gas-phase reaction between OH^- and complex **1** produces a stable carbanion, $\text{MeS}(\text{BH}_3)\text{CH}_2^-$ (**1a**), that does not isomerize under thermal conditions at room temperature to either of the lower energy borate isomers $\text{MeSCH}_2\text{BH}_3^-$ (**1b**) and $\text{CH}_3\text{CH}_2\text{SBH}_3^-$ (**1c**). The structure of **1a** was determined by tandem mass spectrometry and by ion/molecule reactions. The barriers for rearrangement of **1a** to **1b** and to **1c** were calculated to be 29.3, and 27.6 kcal/mol, respectively, at the G2-(MP2) level. The stable carbanions $\text{Me}_2\text{N}(\text{BH}_3)\text{CH}_2^-$ (**2a**), $\text{Me}_2\text{P}(\text{BH}_3)\text{CH}_2^-$ (**3a**), and $\text{MeS}(\text{BF}_3)\text{CH}_2^-$ (**4a**) were also generated by proton abstraction from the corresponding neutral complexes. The gas-phase acidities (ΔH_{acid}) of **1–3** were determined from bracketing experiments to be 372.5 ± 2.0 , 393.0 ± 2.0 , and 374.5 ± 2.0 kcal/mol, respectively. Compared to their uncomplexed bases, the acidities of **1–3** are enhanced by 18–20 kcal/mol. The acidity enhancements were shown to be mainly due to the increased electron binding energies of the carbanions in the deprotonated complexes that result from electrostatic interactions with the strongly dipolar Lewis acid–base bonds. Enhanced reactivity of the Lewis acid–base complexes was also characterized. The complexes **1**, **2**, and Me_2OBF_3 undergo nucleophilic substitution at carbon with F^- or NH_2^- , while no such reactions occur for the uncomplexed bases Me_2S , Me_3N , and Me_2O . Similarly, facile β -elimination reactions occur between F^- or OH^- and the ethylated complexes Et_3NBH_3 and Et_2OBF_3 , while the uncomplexed species are unreactive.

Introduction

It has been nearly two centuries since the first coordination complex, H_3NBF_3 , was made by Gay-Lussac in 1809.¹ The nature of the donor–acceptor bonds in these complexes was described by Lewis beginning in 1923,² and this topic has since been the subject of extensive experimental and theoretical scrutiny.³ The important role of Lewis acid–base complexes in chemical reactions has been recognized and exploited for decades. Many different kinds of complexes have been synthesized and used as reagents and as catalysts to accelerate organic, organometallic, and biochemical reactions.⁴ Modern versions of such catalysts that incorporate chiral Lewis acids constitute a powerful means for asymmetric induction.⁵ A key component of the general mechanism for Lewis acid catalysis is the coordination of the substrate and the resulting activation of its reactive site(s).⁶ This activation may take the form of, inter alia, enhanced electrophilicity of a carbonyl group,⁷ increased Brønsted acidity of α -CH bonds,⁸ or amplified

dienophilicity of an alkenyl moiety within the substrate.⁹ Although there is a wealth of experimental information bearing on how the interaction with a Lewis acid can modify the reactivity and conformational properties of a molecule, little quantitative information is available on the extent to which the thermochemical properties of a compound are changed upon complexation with a Lewis acid. Comparisons of the heterolytic and homolytic bond strengths and the oxidation–reduction potentials of groups within a Lewis acid–base complex with those of the separate molecular components can provide valuable insights into the nature of Lewis acid activation. For example, Lewis-acid-catalyzed aldol condensations have long been used in organic synthetic procedures.^{4c} A key step in these reactions involves the Lewis-acid-promoted enolization of the aldehyde or ketone substrate with a tertiary amine base,¹⁰ which implies an enhancement in the acidity of the α -CH bonds in the carbonyl

(1) Gay-Lussac, J. L.; Thénard, J. L. *Mem. Phys. Chim. d'Arcueil* **1809**, 2, 210.

(2) Lewis, G. N. *Valence and the Structure of Atoms and Molecules*; The Chemical Catalog Co., Inc.: New York, 1923.

(3) (a) Stone, F. G. A. *Chem. Rev.* **1958**, 58, 101. (b) Satchell, D. P. N.; Satchell, R. S. *Chem. Rev.* **1969**, 69, 251. (c) Guryanova, E. N.; Goldshtein, I. P.; Romm, I. P. *The Donor–Acceptor Bond*; Wiley: New York, 1975. (d) Jensen, W. B. *The Lewis Acid–Base Concepts*; Wiley: New York, 1980. (e) Haaland, A. *Angew. Chem., Int. Ed. Engl.* **1989**, 28, 992. (f) Drago, R. S. *Applications of Electrostatic-Covalent Models in Chemistry*; Surfside Scientific: Gainesville, FL, 1994. (g) Jonas, V.; Frenking, G.; Reetz, M. T. *J. Am. Chem. Soc.* **1994**, 116, 8741.

(4) (a) *Metal Sites in Proteins and Models*, Vol. 89; Hill, H. A. O., Sadler, P. J., Thomson, A. J., Eds.; Springer: Berlin, 1997. (b) *Selectivities in Lewis Acid Promoted Reactions*; Schinzer, D., Ed.; Kluwer Academic Publishers: Dordrecht, The Netherlands, 1988. (c) Mukaiyama, T. In *Organic Reactions*, Vol. 28; Dauben, W. G., Ed.; Wiley: New York, 1982; Chapter 4.

(5) (a) Hayashi, Y.; Rohde, J. J.; Corey, E. J. *J. Am. Chem. Soc.* **1996**, 118, 5502. (b) Evans, D. A.; Murry, J. A.; Kozlowski, M. C. *J. Am. Chem. Soc.* **1996**, 118, 5814. (c) Ishihara, K.; Kurihara, H.; Yamamoto, H. *J. Am. Chem. Soc.* **1996**, 118, 3049. (d) Evans, D. A.; Murry, J. A.; von Matt, P.; Norcross, R. D.; Miller, S. J. *Angew. Chem., Int. Ed. Engl.* **1995**, 34, 789. (e) Corey, E. J.; Cimprich, K. A. *J. Am. Chem. Soc.* **1994**, 116, 3151. (f) Corey, E. J.; Letavic, M. A. *J. Am. Chem. Soc.* **1995**, 117, 9616.

(6) (a) Maruoka, K.; Yamamoto, H. In *Catalytic Asymmetric Synthesis*; Ojima, I., Ed.; VCH: New York, 1993. (b) Yamamoto, H.; Maruoka, K.; Furuta, K. In *Selectivities in Lewis Acid Promoted Reactions*; Schinzer, D., Ed.; Kluwer Academic Publishers: Dordrecht, The Netherlands, 1988; p 281. (c) Deloux, L.; Srebnik, M. *Chem. Rev.* **1993**, 93, 763. (d) Yamamoto, Y. *Acc. Chem. Res.* **1987**, 20, 243.

(7) (a) Nishigaichi, Y.; Takuwa, A. *Tetrahedron* **1993**, 49, 7395. (b) Corey, E. J.; Bakshi, R. K.; Shibata, S. *J. Am. Chem. Soc.* **1987**, 109, 5551.

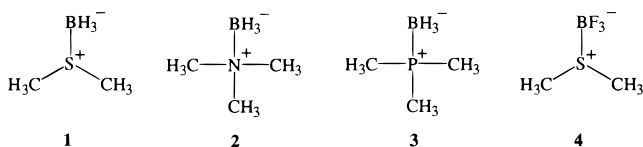
(8) (a) Kessar, S. V.; Singh, P. *Chem. Rev.* **1997**, 97, 721. (b) Vedejs, E.; Kendall, J. T. *J. Am. Chem. Soc.* **1997**, 119, 6941.

(9) Kagan, H. B.; Riant, O. *Chem. Rev.* **1992**, 92, 1007.

(10) (a) Paterson, I. *Pure Appl. Chem.* **1992**, 64, 1821. (b) Evans, D. A.; Nelson, J. V.; Vogel, E.; Taber, T. R. *J. Am. Chem. Soc.* **1981**, 103, 3099.

complex by about 10 pK_a units. This phenomenon raises several important questions: To what extent does Lewis acid complexation increase the intrinsic acidity of the α-CH bonds, and to what extent is the enhancement influenced by solvation? What is the nature of the acidity enhancement?¹¹ Are the kinetic and thermodynamic acidities correlated? Is the increase in acidity a simple function of the complexation energy?¹² We are developing quantitative models for Lewis acid activation that address these questions by using gas-phase ion chemistry techniques to determine the changes in fundamental physical properties such as acidity, basicity, electron affinity, and bond energy that accompany coordination of molecules by Lewis acids. In this paper, we present gas-phase experimental and theoretical studies of a series of prototype Lewis acid–base complexes composed of peralkylated n-donor bases and the common Lewis acids BH₃ and BF₃.

In the course of our earlier investigations of the properties and reactivity of diborane and borohydride ions using the flowing afterglow method,¹³ we explored the utility of borane–dimethyl sulfide complex, Me₂SBH₃ (**1**), as a convenient source of the diborane for gas-phase ion/molecule reactions. The commercially available solutions of borane–dimethyl sulfide (1–10 M in Me₂S) contain sufficient diborane in their head vapors at room temperature for practical use in flowing afterglow experiments. However, in using this material, we found that not only was the borane–dimethyl sulfide complex itself sufficiently volatile and reactive to display ion/molecule reactions in the flow tube, but also it was much more acidic in the Brønsted sense than uncomplexed dimethyl sulfide. That is, an apparent proton-transfer product, C₂H₃BS[−], was observed in reactions of borane–dimethyl sulfide complex with negative ions that are too weakly basic to deprotonate dimethyl sulfide. These observations led us to investigate the gas-phase acidity of **1** and related Lewis acid–base complexes, as well as the structures and reactivity of the ions produced by deprotonation.¹⁴ In this work, we demonstrate that removal of a methyl proton from the BH₃ and BF₃ complexes of dimethyl sulfide (**1** and **4**, respectively) and the BH₃ complexes of trimethylamine (**2**) and trimethylphosphine (**3**) produces novel dipole-stabilized carbanions, and that the gas-phase acidities of the borane complexes



are enhanced relative to the uncomplexed molecules by as much as 20 kcal/mol. We also show that the alkyl groups in **1–4** and other borane complexes are strongly activated toward gas-phase nucleophilic substitution and elimination reactions with negative ions. The structures and thermochemical properties of **1**, its conjugate base anion, and related species have also been examined in detail with ab initio molecular orbital calculations carried out at the G2(MP2)¹⁵ and CBS-4¹⁶ levels of theory.

(11) (a) Wiberg, K. B.; Ochterski, J.; Streitwieser, A. *J. Am. Chem. Soc.* **1996**, *118*, 8291. (b) Bordwell, F. G.; Satish, A. V. *J. Am. Chem. Soc.* **1994**, *116*, 8885.

(12) Anane, H.; Boutalib, A.; Tomás, F. *J. Phys. Chem. A* **1997**, *101*, 7879.

(13) (a) Workman, D. B.; Squires, R. R. *Inorg. Chem.* **1988**, *27*, 1846. (b) Workman, D. B. Ph.D. Thesis, Purdue University, 1989.

(14) Ren, J.; Workman, D. B.; Squires, R. R. *Angew. Chem., Int. Ed. Engl.* **1997**, *36*, 2230.

(15) Curtiss, L. A.; Raghavachari, K.; Pople, J. A. *J. Chem. Phys.* **1993**, *98*, 1293.

Experimental Section

All experiments were carried out at room temperature with a flowing afterglow triple-quadrupole instrument that is described elsewhere.¹⁷ Unless otherwise noted, the total pressure and flow rate of the helium buffer gas used were 0.4 Torr and 190 STP cm³/s, respectively. Hydroxide ions were formed by electron ionization of a N₂O/CH₄ mixture, while NH₂[−] and F[−] were produced by electron ionization of NH₃ and NF₃, respectively. Other negative ions were formed by reaction of one of the above bases with the corresponding neutral conjugate acids. Product distributions for ion/molecule reactions in the flow tube were determined either directly from the mass spectra when secondary reactions did not occur or from the slopes of plots of the product ion yields versus the extent of reactant ion conversion. For ion/molecule reaction studies, the detector resolution was kept as low as practical so as to minimize mass discrimination.

Collision-induced dissociation (CID) measurements and mass-selected ion/molecule reactions were carried out in the gas-tight, radio-frequency-only quadrupole collision chamber (Q2) of the triple-quadrupole mass analyzer. Argon target gas was used for the CID experiments, with pressures ranging from 0.04 to 0.12 mTorr. The axial kinetic energy of the reactant ion is determined by the Q2 rod offset voltage, which can be varied up to 200 V. For studies of exothermic ion/molecule reactions taking place in Q2, the offset voltage and ion extraction voltages were maintained as low as practical (<0.5 V) to approximate thermal energy conditions. The methods used for measurement and analysis of CID threshold energies have been described in detail previously.¹⁸ Briefly, the cross section for dissociation of the mass-selected reactant ion is measured as a function of the collision energy in the center-of-mass frame, with argon target maintained in Q2 at pressures less than 0.05 mTorr. The product ion appearance curves are fit with an analytical model that takes into account the ion beam kinetic energy spread, the Doppler broadening due to target motion, the internal energy content of the reactant ion (assumed to be at a temperature of 298 K), and kinetic shifts due to slow dissociation on the instrument time scale.¹⁹ The vibrational frequencies required for the internal energy and kinetic shift calculations were obtained from ab initio molecular orbital calculations carried out at the B3LYP/6-31G(d) level without scaling.

Materials. Gas purities were as follows: He(99.995%), Ar-(99.955%), N₂O(99%), CH₄(99%), NH₃ (anhydrous, 99.5%), NF₃(99%), CO₂ (99.5%). Borane dimethyl sulfide (10 M in Me₂S), trifluoroborane dimethyl sulfide, borane trimethylamine, borane triethylamine, trifluoroborane dimethyl ether, trifluoroborane diethyl ether, and trifluoroborane tetrahydrofuran were obtained from Aldrich Chemical Co. and used as supplied. Borane trimethylphosphine was produced by mixing pure trimethylphosphine with a 1 M solution of borane in tetrahydrofuran. Removal of the excess tetrahydrofuran by distillation yields the pure complex as a volatile crystalline solid. Borane-*d*₃-dimethyl sulfide, Me₂SBD₃, was prepared by bubbling B₂D₆²⁰ into Me₂S. All other reagents were obtained from commercial vendors and used as supplied except for degassing of liquid samples prior to use.

Computational Details. The structures and energies of complexes **1–4**, their conjugate base anions, and a series of related anions and neutral molecules were calculated with use of the G2(MP2)¹⁵ and CBS-4¹⁶ procedures. For G2(MP2) calculations, optimized geometries are obtained at the MP2(full)/6-31G(d,p) level of theory, and harmonic vibrational frequencies for the zero-point energy and temperature corrections are determined at the HF/6-31G(d) level and scaled by a

(16) Ochterski, J. W.; Petersson, G. A.; Montgomery, J. A. *J. Chem. Phys.* **1996**, *104*, 2598.

(17) (a) Graul, S. T.; Squires, R. R. *Mass Spectrom. Rev.* **1988**, *7*, 263. (b) Marinelli, P. J.; Paulino, J. A.; Sunderlin, L. S.; Wenthold, P. G.; Poutsma, J. C.; Squires, R. R. *Int. J. Mass Spectrom. Ion Processes* **1994**, *130*, 89.

(18) (a) Sunderlin, L. S.; Wang, D.; Squires, R. R. *J. Am. Chem. Soc.* **1992**, *114*, 2788. (b) Sunderlin, L. S.; Wang, D.; Squires, R. R. *J. Am. Chem. Soc.* **1993**, *115*, 12060.

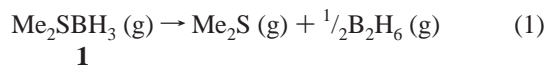
(19) Data analysis was carried out with the CRUNCH program developed by P. B. Armentrout and K. M. Ervin.

(20) The synthetic procedure was adapted from Brown, H. C.; Midland, M. M. In *Organic Synthesis via Boranes*; Wiley-Interscience: New York, 1975; pp 18–21.

factor of 0.893. Single-point energy calculations with each of the MP2-optimized geometries are carried out at higher levels of theory, and an additivity scheme given by Pople et al.¹⁵ is used to derive estimated total energies at the QCISD(T)/6-311+G(3df,2p) level. The CBS-4 procedure utilizes optimized geometries and vibrational frequencies obtained at the HF/3-21G(d) level of theory (frequency scale factor = 0.9167) and an extrapolation scheme based on higher-level calculations to estimate the total energy corresponding to the complete basis set limit.¹⁶ All calculations were carried out with the GAUSSIAN 92²¹ and GAUSSIAN 94²² suites of programs.

Results

Borane–Dimethyl Sulfide and Trifluoroborane–Dimethyl Sulfide. Borane–dimethyl sulfide complex (**1**) forms reversibly in solutions of diborane in neat dimethyl sulfide. These solutions are commercially available as convenient sources of BH₃ for organic synthesis. Stone and co-workers determined the enthalpy and entropy of dissociation of **1** in the gas phase to be 6.1 ± 0.5 kcal/mol and 18.0 eu, respectively, by variable-temperature saturation-pressure tensimetry.²³ Therefore, at 298 K, **1** is 53% dissociated to dimethyl sulfide and diborane (eq 1). Combining the measured enthalpy change for reaction 1 with an updated value for the 298 K dimerization enthalpy of borane²⁴ gives a value for $DH_{298}[\text{Me}_2\text{S}-\text{BH}_3]$ of 25.9 kcal/mol.



Reaction in the room-temperature flow tube between OH[−] and the head vapors sampled from a 10 M solution of borane–dimethyl sulfide in Me₂S produces a host of negative ion products derived from diborane and the volatile complex, **1**. These include BH₄[−] and polyborohydride anions B_nH_m[−] (*n* = 2–4; *m* = 5–10), the apparent proton abstraction product C₂H₈BS[−] (eq 2), and its borane adduct C₂H₈BS(BH₃)[−], probably



formed as a secondary product (vide infra). BH₄[−] and polyborohydrides have been observed previously in gas-phase reactions of OH[−] (and other negative ions) with pure diborane.²⁵ The proton-transfer product is of particular interest, since OH[−] is too weakly basic to deprotonate dimethyl sulfide (the main constituent of the head vapors) at a significant rate in the gas phase at room temperature ($\Delta H_{\text{acid}}(\text{H}_2\text{O}) = 390.7$ kcal/mol; $\Delta H_{\text{acid}}(\text{Me}_2\text{S}) = 393.2$ kcal/mol).²⁶ This rules out the formation

(21) Frisch, M. J.; Trucks, G. W.; Schlegel, H. B.; Gill, P. M. W.; Johnson, B. G.; Wong, M. W.; Foresman, J. B.; Robb, M. A.; Head-Gordon, M.; Replogle, E. S.; Gomperts, R.; Andres, J. L.; Binkley, K.; Raghavachari, J. S.; Gonzalez, C.; Martin, R. L.; Fox, D. J.; Defrees, D. J.; Baker, J.; Stewart, J. J. P.; Pople, J. A. *Gaussian 92/DFT*, Revision G.3; Gaussian, Inc.: Pittsburgh, PA, 1993.

(22) Frisch, M. J.; Trucks, G. W.; Schlegel, H. B.; Gill, P. M. W.; Johnson, B. G.; Robb, M. A.; Cheseseaman, J. R.; Keith, T.; Petersson, G. A.; Montgomery, J. A.; Raghavachari, K.; Al-Laham, M. A.; Zakrzewski, V. G.; Ortiz, J. V.; Foresman, J. B.; Cioslowski, J.; Stefanov, B. B.; Nanayakkara, A.; Challacombe, M.; Peng, C. Y.; Ayala, P. Y.; Chen, W.; Wong, M. W.; Andres, J. L.; Replogle, E. S.; Gomperts, B.; Martin, R. L.; Fox, D. J.; Binkley, J. S.; Defrees, D. J.; Baker, J.; Stewart, J. J. P.; Head-Gordon, M.; Gonzalez, C.; Pople, J. A.; *Gaussian 94*, ver. D.2, Gaussian, Inc.: Pittsburgh, PA, 1995.

(23) Coyle, T. D.; Kaesz, H. D.; Stone, F. G. A. *J. Am. Chem. Soc.* **1959**, *81*, 2989.

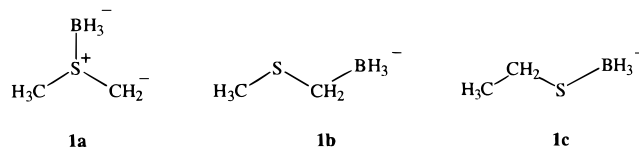
(24) Page, M.; Adams, G. F.; Binkley, J. S.; Melius, C. F. *J. Phys. Chem.* **1987**, *91*, 2675.

(25) (a) Eisenstein, O.; Kayser, M.; Roy, M.; McMahon, T. R. *Can. J. Chem.* **1985**, *63*, 281. (b) Dunbar, R. C. *J. Am. Chem. Soc.* **1968**, *90*, 5670.

(26) Lias, S. G.; Bartmess, J. E.; Liebmann, J. F.; Holmes, J. L.; Levin, R. D.; Mallard, W. G. *J. Phys. Chem. Ref. Data* **1988**, *17*, Suppl 1. Updated in J. E. Bartmess, NIST Std. Ref. Database 19B (Negative Ion Energetics Database ver. 3.00), 1993.

of C₂H₈BS[−] by a stepwise mechanism in which uncomplexed Me₂S is first deprotonated, followed by reaction of the resulting carbanion with diborane.

We consider three plausible structures for the C₂H₈BS[−] ion formed by reaction 2. Deprotonation of Me₂SBH₃ (**1**) at carbon can give a carbanion **1a** in which the S–B bond is maintained. Alternatively, rearrangement by a formal [1,2]-BH₃ shift or a [1,2]-CH₃ shift produces isomers **1b** and **1c**, respectively. The



latter two isomers are predictably lower energy forms, since the carbon lone pair in MeSCH₂[−] is much more basic than the sulfur lone pairs, and CH₃CH₂S[−] is 40 kcal/mol more stable than CH₃SCH₂[−].²⁶ In fact, ab initio calculations carried out at the G2(MP2) level of theory predict that **1b** and **1c** are lower in energy than **1a** by 28 and 44 kcal/mol, respectively. We have used a combination of CID and ion/molecule reactions to identify the structure of the reaction product as **1a**. For comparison, ions with authentic structures **1b,c** were generated by allowing deprotonated dimethyl sulfide (produced from NH₂[−] + Me₂S) and ethanethiolate anion (produced from F[−] + EtSH) to react with diborane (eqs 3 and 4).

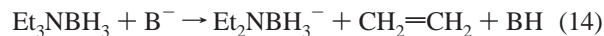


The CID spectra of the C₂H₈BS[−] ions produced by reactions 2–4 are shown in Figure 1, parts a–c, respectively. The three spectra are qualitatively distinct. Methyl loss is the dominant fragmentation of the ion produced by deprotonation of **1** ($\sigma_{\text{max}} = 5$ Å²), while it is only a minor channel for ion **1b** ($\sigma_{\text{max}} = 1$ Å²). Similarly, formation of CH₃S[−] represents the major dissociation for **1b** ($\sigma_{\text{max}} = 4$ Å²) but is only a minor process for the conjugate base of **1**. Isomer **1c** displays only a single fragment ion, CH₃CH₂S[−], which results from BH₃ loss. The yield for BH₃ cleavage from **1b** is about half that from **1a**. We find no significant pressure dependence of the relative differences among the three CID spectra, which suggests that isomerization of **1a** to **1b** or **1c** is not induced by multiple-collision conditions. The qualitative differences among the spectra leave little doubt that the ions (or ion mixtures) produced by reactions 2–4 are different.

Ion/molecule reactions tell a similar story. The ion produced by deprotonation of **1** reacts with both D₂O and CH₃OD by exchange of up to five hydrogens for deuterium. This behavior is consistent with structure **1a**, which has five exchangeable hydrogens, and with the well-established mechanism for gas-phase H/D exchange in carbanions.²⁷ In contrast, ions **1b,c** do not react at all with added D₂O or CH₃OD. This is the expected behavior for substituted borohydride ion such as **1b,c**, which do not possess any hydrogen-bearing, Brønsted basic sites. It is noteworthy that deprotonated dimethyl sulfide, MeSCH₂[−], also does not undergo exchange with either D₂O or CH₃OD,

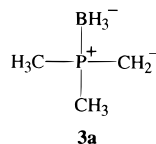
(27) (a) Stewart, J. H.; Shapiro, R. H.; DePuy, C. H.; Bierbaum, V. M. *J. Am. Chem. Soc.* **1977**, *99*, 7650. (b) DePuy, C. H.; Bierbaum, V. M.; King, G. K.; Shapiro, R. H. *J. Am. Chem. Soc.* **1978**, *100*, 2921.

The behavior of borane–triethylamine, Et_3NBH_3 , illustrates another mode of enhanced reactivity of the amine in a borane–amine complex. Reaction in the flow tube between either OH^- or F^- and the head vapors sampled from pure borane triethylamine complex yields exclusively the elimination product $\text{Et}_2\text{NBH}_3^-$ (eq 14, $\text{B}^- = \text{OH}^-$ or F^-). A β -elimination rather



than $\text{S}_{\text{N}}2$ substitution mechanism for Et_3NBH_3 is indicated by the fact that the analogous product, $\text{Me}_2\text{NBH}_3^-$, is not observed when either OH^- or F^- reacts with Me_3NBH_3 . Hydroxide-induced elimination of ethylene from uncomplexed triethylamine is endothermic by about 14 kcal/mol²⁶ and does not occur in the gas phase. Thus, coordination of triethylamine by BH_3 activates the ethyl groups toward Hoffmann-like β -elimination reactions.

Borane–Trimethylphosphine. The use of borane–trialkylphosphine complexes and their α -lithiated derivatives as novel reagents for asymmetric synthesis was recently reported by Evans and co-workers.⁴¹ Equilibrium studies⁴² show that the P–B bond strength in borane–trimethylphosphine complex **3** is greater than the N–B bond strength in **2**, so **3** will also remain undissociated in the gas phase at room temperature. Reaction of complex **3** and OH^- proceeds entirely by proton transfer. Carbanion structure **3a** is assigned to the product based on the



observed reactivity, i.e., it undergoes up to 8 H/D exchanges upon reaction with D_2O , and reacts with both CO_2 and BEt_3 to yield adducts but no electrophilic substitution products. The absence of electrophilic substitution in this case is probably due to the exceptionally strong P–B bond in ion **3a**. CID of **3a** at 3.5 eV (center-of-mass) gives $\text{Me}_2\text{PCH}_2^-$ as the only ionic product.

Acid–base bracketing experiments show the acidity of **3** to be between that of DMSO ($\Delta G_{\text{acid}} = 366.4 \pm 2.0$ kcal/mol²⁶) and $\text{FCH}_2\text{CH}_2\text{OH}$ ($\Delta G_{\text{acid}} = 364.6 \pm 0.4$ kcal/mol²⁶), from which we assign $\Delta G_{\text{acid}}(\mathbf{3}) = 365.5 \pm 2.0$ kcal/mol. Combining this with an estimate for $\Delta S_{\text{acid}}(\mathbf{3})$ of 30.4 eu gives $\Delta H_{\text{acid}}(\mathbf{3}) = 374.5 \pm 2.0$ kcal/mol. Compared to trimethyl phosphine ($\Delta H_{\text{acid}} = 391.1 \pm 2.1$ kcal/mol⁴³), the BH_3 complex **3** is a stronger acid by 17 kcal/mol.

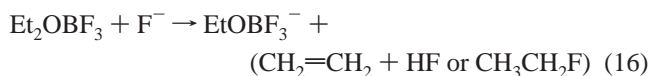
Trifluoroborane–Etherates. Trifluoroborane–etherate complexes, R_2OBF_3 , typically formed as dilute (<1 M) solutions in the corresponding ether, are common sources of BF_3 for use in synthesis. The O–B bond strengths in these complexes are in the range 10–20 kcal/mol.³ We briefly examined the gas-phase negative ion chemistry of the BF_3 complexes of three simple ethers: dimethyl ether, diethyl ether, and tetrahydrofuran (THF).

Reaction of the head vapors sampled from pure Me_2OBF_3 with either NH_2^- or OH^- does not produce an observable proton

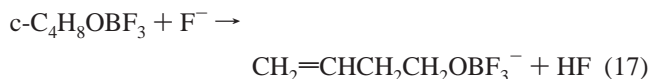
abstraction product. Rather, only primary and secondary product ions derived from reactions of free BF_3 are produced, including BF_4^- , BF_2O^- , and $\text{F}_2\text{BOBF}_3^-$. In contrast, when F^- is the reactant ion, nucleophilic substitution is observed to yield MeOBF_3^- (eq 15). This product cannot have arisen by a



stepwise process in which F^- first reacts with Me_2O to produce MeO^- which then adds to free BF_3 , since uncomplexed Me_2O does not react with F^- at all. Therefore, as with **1–4**, it must be a unique reaction of the Me_2OBF_3 complex in which borane coordination activates the methyl groups toward nucleophilic attack. Reaction of F^- with trifluoroborane–diethyl ether, Et_2OBF_3 , produces exclusively the analogous product ion EtOBF_3^- , while uncomplexed Et_2O does not react with F^- under the same conditions. The observed product ion could arise by either α -substitution or β -elimination (eq 16). These two possibilities



are distinguishable with cyclic ethers, since the masses of the substitution and elimination products are different. Accordingly, the reaction of F^- with trifluoroborane–tetrahydrofuran complex, $\text{c-C}_4\text{H}_8\text{OBF}_3$, was examined. A single product ion is observed corresponding to $\text{C}_4\text{H}_7\text{OBF}_3^-$, which is consistent with the occurrence of elimination (eq 17) but not substitution. This same preference for elimination over substitution has been deduced from studies of the gas-phase reactions of OH^- and NH_2^- with the uncomplexed ethers.⁴⁴



Computational Results. The geometries, electronic structures, and thermochemical properties of borane and trifluoroborane complexes, their conjugate base anions, and a series of related ions and neutral molecules were examined computationally using G2(MP2) and CBS-4 procedures. In addition, the transition structures, **TS1ab**, linking isomers **1a** and **1b** and **TS1ac** linking isomers **1a** and **1c** were also characterized at the G2(MP2) level, and the conformational properties of **1a** were examined with an MP2(fc)/6-31+G(d) procedure.

Optimized structural parameters obtained at the MP2(full)/6-31G(d,p) and MP2(fc)/6-31G(d) levels for selected species from the dimethyl sulfide series (**1** and **4**) are summarized in Figure 2. Full geometrical descriptions and listings of total energies for each of these species are given along with data for **2**, **3**, and related molecules in the Supporting Information. Coordination of Me_2S by either BH_3 or BF_3 leads to relatively small structural changes in the components of each complex. Optimized S–B bond distances of 1.99 and 2.15 Å are computed for **1** and **4**, respectively. The S–C bond distances and CSC bond angles in the Me_2S moieties are about the same as in the free molecule, and the borane fragments in the complexes are relatively little pyramidalized.

Deprotonation of **1** and **4** leads to pronounced structural changes. The computed structures for **1** and **1a** indicate that the S– CH_2 bond length decreases by 0.06 Å upon deprotonation, while the S– CH_3 bond length increases by 0.02 Å. These

(41) Muci, A. R.; Campos, K. R.; Evans, D. A. *J. Am. Chem. Soc.* **1995**, *117*, 9075.

(42) Young, D. E.; McAchran, G. E.; Shore, S. G. *J. Am. Chem. Soc.* **1966**, *88*, 4390.

(43) Ingemann, S.; Nibbering, N. M. M. *J. Chem. Soc., Perkin Trans. 2* **1985**, 837. A somewhat lower value for $\Delta H_{\text{acid}}(\text{Me}_3\text{P})$ is given by Grabowski et al. (Grabowski, J. J.; Roy, P. D.; Leone, R. *J. Chem. Soc., Perkin Trans. 2* **1988**, 1627).

(44) (a) DePuy, C. H.; Bierbaum, V. M. *J. Am. Chem. Soc.* **1981**, *103*, 5034. (b) DePuy, C. H.; Beedle, E. C.; Bierbaum, V. M. *J. Am. Chem. Soc.* **1982**, *104*, 6483.

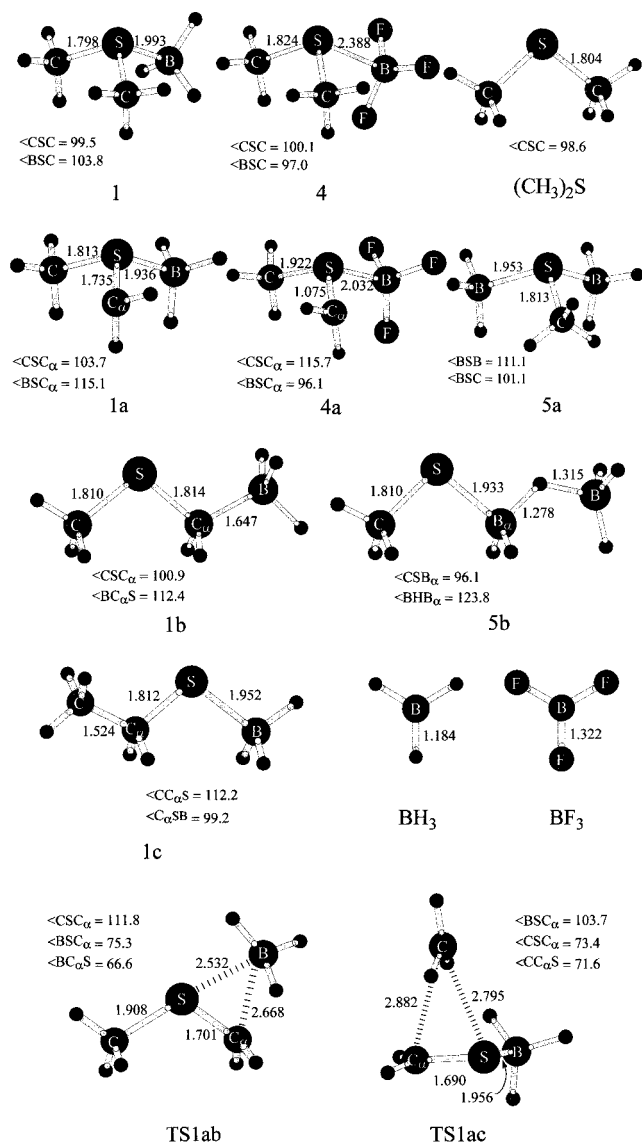


Figure 2. Optimized structures for selected molecules related to complexes **1** and **4**. Geometries determined at the MP2(full)/6-31G(d,p) level for all species except **4** and **4a**, which were determined at the MP2(fc)/6-31G(d) level.

structural changes are similar to those calculated for deprotonation of uncomplexed dimethyl sulfide and dimethyl sulfoxide.⁴⁵ X-ray structures of sulfur ylides also indicate that the ylide carbon–sulfur bond length tends to be shorter than a normal S–C single bond.⁴⁶ The calculations also indicate a shorter S–B bond and a more pyramidalized BH₃ moiety in **1a** compared to **1**. The CH₂ group in **1a** is quite pyramidal and adopts a conformation such that one of its hydrogens eclipses the S–B bond and the lone pair is gauche to the S–C bond. This conformation minimizes repulsion among the carbanion lone pair, the sulfur lone pair, and the negatively charged BH₃ group. The energy profile for rotation about the S–CH₂ bond in **1a** was examined at the MP2(fc)/6-31+G(d) level of theory and is shown in Figure 3. Rotation with full relaxation of all degrees of freedom gives rise to the energy profile shown as the dotted line. For torsional angles Φ greater than about 170°, inversion

(45) (a) Speers, P.; Laidig, K. E.; Streitwieser, A. *J. Am. Chem. Soc.* **1994**, *116*, 9257. (b) Wiberg, K. B.; Castejon, H. *J. Am. Chem. Soc.* **1994**, *116*, 10489.

(46) Trost, B. M.; Melvin, L. S., Jr. *Sulfur Ylides*; Academic Press: New York, 1975; Chapter 3.

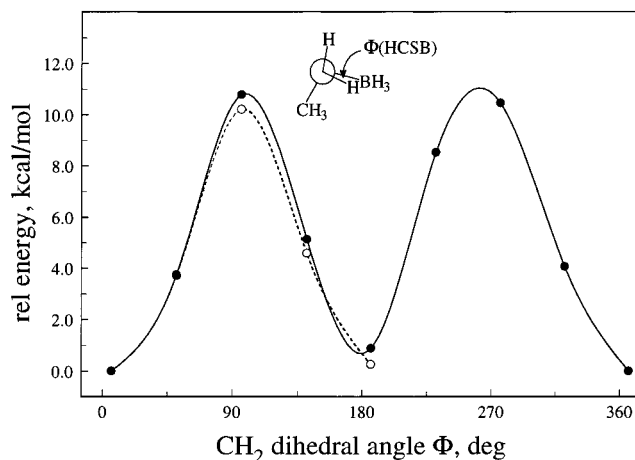


Figure 3. Calculated energy profile for clockwise rotation about the S–CH₂ bond in carbanion **1a**. Relative energies for selected conformers computed at the MP2(fc)/6-31+G(d) level are indicated by the solid and open circles, and the smooth curves are spline fits of the data. Rotation energy profile with full relaxation in all other coordinates shown as the dotted line; rotation of rigid CH₂ group maintained at its initial ($\Phi = 0^\circ$) local geometry indicated by the solid line.

of the CH₂ group occurs during geometry optimization. The torsional energy profile for rotation of a rigid CH₂ group maintained at its initial ($\Phi = 0^\circ$) local geometry was also computed and is shown as the solid line in Figure 3. The two ca. 11 kcal/mol maxima at $\Phi \approx 90^\circ$ and $\Phi \approx 270^\circ$ correspond to eclipsing of the carbanion lone pair with the sulfur lone pair and the S–B bond, respectively.

Similar geometrical changes are also found in the BF₃ complexed species, **4** and **4a**, except that the CH₂ in **4a** is pyramidalized with the lone pair oriented gauche to the BF₃ group in the lowest energy conformer. The carbanion–BX₃ repulsive interaction is smaller in **4a** compared to **1a** since the S–B bond is longer. Moreover, in the preferred conformation of **4a**, the lone pair on CH₂ is anti-periplanar to the S–CH₃ bond, thereby enabling negative hyperconjugation with the S–CH₃ σ^* orbital.^{45b} The **4a** conformation with the carbanion lone pair gauche to the S–C bond (analogous to the preferred conformation of **1a**) is only 1.2 kcal/mol higher in energy.

Natural bond orbital (NBO) analysis⁴⁷ indicates the CH₂ group to have the greatest negative charge density in both **1a** and **4a**. A summary of the net charge shifts that accompany deprotonation of **1** and **4** is given in Table 1. In going from **1** to **1a**, the charge at the α -carbon increases by 0.76 e (similar to the computed charge shift for deprotonation of DMSO^{45b}), while the charge density at sulfur remains essentially unchanged and the charge shifts to the BH₃ and CH₃ groups are small. The change of the charge distribution in going from **4** to **4a** shows a similar pattern, but with a distinctly greater polarization of the S–BF₃ bond due to the greater electronegativity of fluorine compared to hydrogen.

Isomers **1b,c** have structures consistent with a designation as strongly bonded “ate” complexes. The B–C bond distance in **1b** is 1.65 Å, only 0.14 Å longer than that in lithium tetramethylborate,⁴⁸ and the BH₃ moiety is fully pyramidalized with a staggered conformation. Similarly, the B–S distance in **1c** is 1.95 Å and the BH₃ group is pyramidal.

The optimized transition structure **TS1ab** for the isomerization from **1a** to **1b** by a [1,2]-BH₃ shift involves a nearly-

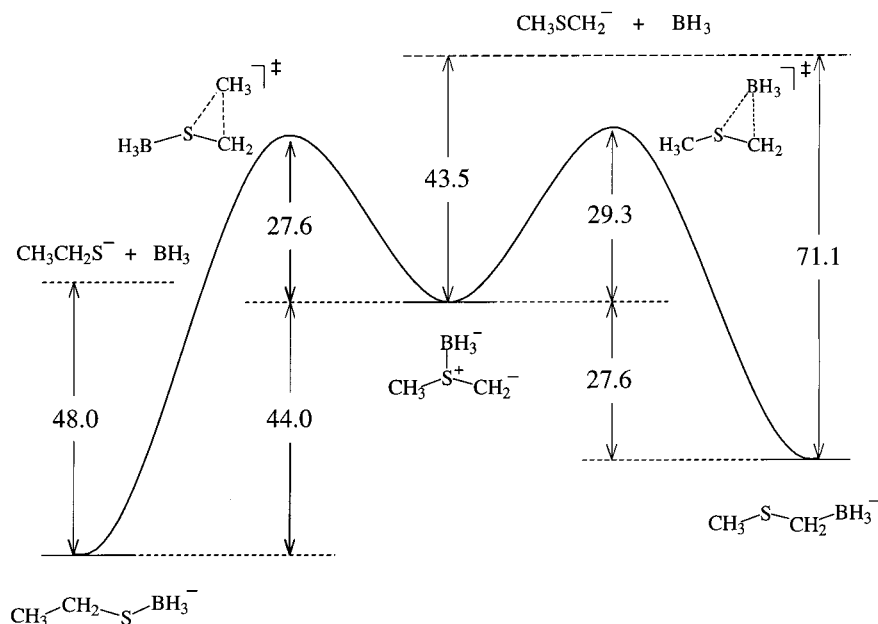
(47) Weinhold, F.; Carpenter, J. E. *The Structure of Small Molecules and Ions*; Plenum Press: New York, 1988.

(48) Groves, D.; Rhine, W.; Stucky, G. D. *J. Am. Chem. Soc.* **1971**, *93*, 1553.

Table 1. Calculated Charge Distributions and Charge Shifts from NBO Analysis

group	Me ₂ SBH ₃ (1) ^a	MeS(BH ₃)CH ₂ ⁻ (1a) ^a	charge shift	group	Me ₂ SBF ₃ (4) ^b	MeS(BF ₃)CH ₂ ⁻ (4a) ^b	charge shift
S	0.638	0.645	-0.007	S	0.444	0.507	0.063
BH ₃	-0.514	-0.661	-0.147	BF ₃	-0.331	-0.533	-0.202
CH ₃	0.062	-0.165	-0.103	CH ₃	-0.055	-0.209	-0.154
CH ₂ ⁻		-0.818	-0.756	CH ₂ ⁻		-0.766	-0.711

^a MP2(full)/6-31G(d,p) geometry. ^b MP2(fc)/6-31G(d) geometry.

**Figure 4.** G2(MP2) energy profile in kcal/mol for isomerization of **1a** to **1b** and **1c** by a [1,2]-BH₃ shift and a [1,2]-CH₃ shift, respectively.

symmetrical three-membered ring with S–B and B–C distances of 2.53 and 2.67 Å, respectively. The S–CH₂ bond length (1.70 Å) is shorter than that in both **1a** and **1b**, while the S–CH₃ bond is somewhat elongated. The geometries of the MeSCH₂⁻ and BH₃ fragments in **TS1ab** are nearly the same as those of the free species, which means that in the transition state the migrating BH₃ group is only loosely bonded to MeSCH₂⁻. Critical points on the potential energy surface for isomerization of **1a** to **1b** via a [1,2]-borane shift were determined at the G2(MP2) level of theory and are shown in schematic form in Figure 4. The computed transition state was characterized by a single imaginary frequency (405i cm⁻¹) corresponding to motion along the BH₃ migration coordinate, which involves pronounced elongation of the S–B bond accompanied by some rotation of the S–CH₂ bond to accommodate the developing B–C bond. The computed barrier height is 29.3 kcal/mol, placing the transition state for rearrangement 14.2 kcal/mol below the energy required to dissociate **1a** to MeSCH₂⁻ + BH₃. The computed transition structure and high energy barrier for conversion of **1a** to **1b** are consistent with expectations for an orbital symmetry forbidden unimolecular isomerization.⁴⁹

Isomerization of **1a** to **1c** by a [1,2]-CH₃ shift is found to have a barrier of 27.6 kcal/mol (Figure 4). Like **TS1ab**, the optimized transition structure **TS1ac** also involves a nearly-symmetrical three-membered ring and a single imaginary frequency (310i cm⁻¹) corresponding to motion of the migrating group between the sulfur and carbon atoms. However, **TS1ac** has longer bonds to the migrating group (*r*(C–C) = 2.82 Å; *r*(S–C) = 2.80 Å) than **TS1ab**, and an orthogonal orientation of the nearly planar methyl group with respect to a [CH₂SBH₃] substructure that resembles a thioformaldehyde–borane com-

Table 2. Calculated Enthalpy Changes for Selected Reactions at 298 K (kcal/mol)

reaction	ΔH ₂₉₈
Me ₂ SBH ₃ (1) → Me ₂ S + BH ₃	22.6 ^a (25.9) ^c
MeS(BH ₃)CH ₂ ⁻ (1a) → MeSCH ₂ ⁻ + BH ₃	43.5 ^a (46.6) ^d
MeSCH ₂ BH ₃ ⁻ (1b) → MeSCH ₂ ⁻ + BH ₃	71.1 ^a
CH ₃ CH ₂ SBH ₃ ⁻ (1c) → CH ₃ CH ₂ S ⁻ + BH ₃	48.0 ^a
MeSCH ₂ BH ₃ → MeSCH ₂ + BH ₃	18.4 ^a
MeS(BH ₃)CH ₂ ⁻ (1a) → MeSCH ₂ BH ₃ ⁻ (1b)	-27.6 ^a
CH ₃ S(BH ₃)CH ₂ ⁻ (1a) → CH ₃ CH ₂ SBH ₃ ⁻ (1c)	-44.2 ^a
MeS(BH ₃) ₂ ⁻ (5a) → MeS(BH ₃) ⁻ + BH ₃	39.1 ^a
MeSBH ₂ -H-BH ₃ ⁻ (5b) → MeS(BH ₃) ⁻ + BH ₃	26.4 ^a
Me ₂ SBF ₃ (4) → Me ₂ S + BF ₃	9.0 ^b (3.5) ^e
MeS(BF ₃)CH ₂ ⁻ (4a) → MeSCH ₂ ⁻ + BF ₃	35.0 ^b
MeSCH ₂ BF ₃ ⁻ (4b) → MeSCH ₂ ⁻ + BF ₃	70.7 ^b

^a Enthalpy changes calculated at the G2(MP2) level. ^b Enthalpy changes calculated at the CBS-4 level. ^c Experimental value, ref 23. ^d Experimental value from this work, derived from measured gas-phase acidity and the thermochemical cycle illustrated in Scheme 2. ^e Experimental value, ref 33.

plex. The computed geometry and charge distribution obtained for **TS1ac** at the MP2(full)/6-31G(d,p) level are indicative of a Wittig-like [1,2]-methyl anion shift, as opposed to a methyl radical or methyl cation shift.⁵⁰ The group charges in **TS1ac** derived from NBO analysis are CH₃ (-0.35), CH₂ (-0.28), S (0.25), and BH₃ (-0.62). **TS1ac** is quite similar to the transition structure found at the same level of theory for the [1,2]-CH₃ shift in uncomplexed CH₃SCH₂⁻ anion, which also has a relatively low barrier (23.5 kcal/mol) and charge distribution indicative of a methyl anion migration mechanism.

The computed structures for isobaric ions **5a,b** merit comment. The lower energy isomer **5a** incorporates two equivalent S–B bonds, whereas **5b** has a single S–B bond with the other

(49) Woodward, R. B.; Hoffmann, R. *The Conservation of Orbital Symmetry*; Verlag Chemie: Weinheim, Germany, 1970.

(50) Schollkopf, U. *Angew. Chem., Int. Ed. Engl.*, **1970**, *9*, 763.

Table 3. Gas-Phase Acidities, Electron Affinities, and Homolytic Bond Dissociation Enthalpies (kcal/mol)

	Me ₂ SBH ₃	Me ₂ S	Me ₃ NBH ₃	Me ₃ N	Me ₃ PBH ₃	Me ₃ P
$\Delta H_{\text{acid}}(\text{RH})$						
expt	372.5 \pm 2.0 ^a	393.2 \pm 2.1	393.0 \pm 2.0 ^a	>404	374.5 \pm 2.0 ^a	391.1 \pm 2.1
theory	371.8, ^b 372.4	392.7, ^b 392.3	393.9	411.4	373.4	389.6
$\Delta H_{298}[\text{RH}]$						
expt	95.8 \pm 3.0 ^a	96.6 \pm 1.0				
theory	97.9, ^b 102.5	93.7, ^b 94.3	103.4	92.5	102.8	98.3
EA(R)						
expt	36.9 \pm 2.3 ^a	20.0 \pm 1.2		< 0		
theory	39.5, ^b 43.2	14.7, ^b 15.5	23.1	-5.3	42.8	22.3

^a This work, all other experimental data taken from ref 26. ^b G2(MP2) model, all other theoretical results from the CBS-4 model.

Table 4. Comparison of Calculated^a Gas-Phase Acidities for Isoelectronic Model Compounds

compd	ΔH_{acid} , kcal/mol	compd	ΔH_{acid} , kcal/mol
Me ₂ SBH ₃	372.4	Me ₃ NBH ₃	393.9
Me ₂ SO	374.3	Me ₃ NO	389.0
Me ₃ S ⁺	252.6	Me ₃ PBH ₃	373.4
		Me ₃ PO	378.7

^a CBS-4 model.

BH₃ molecule engaged in a hydride-bridging interaction with the coordinated BH₃. This latter structure is similar to those described by Eisenstein et al.⁵¹ for other substituted diborane anions, XB₂H₆⁻ (X = H, F, MeO) and to the neutral Lewis base adducts of diborane described by Sakai⁵² and DiMare.⁵³ The S–B bond distances calculated for **5a,b** are about the same (1.94 Å), despite the differing formal oxidation state of the sulfur atom in the two forms. The ability of sulfur to accommodate two Lewis acid bonding interactions in ion **5a** arises from its large size and the diffuse nature of the lone-pair orbitals in CH₃S⁻.

The 298 K enthalpy changes computed for selected dissociation and isomerization reactions pertinent to the dimethyl sulfide complexes are summarized in Table 2 along with some experimental values for comparison. Values of the gas-phase acidities, homolytic α -CH bond dissociation enthalpies, and radical electron affinities for compounds **1–3** are given in Table 3, along with the available experimental data from the literature and from the present work. Gas-phase acidities for some model compounds that are isoelectronic with **1–3** were determined at the CBS-4 level of theory and are summarized in Table 4. For all of the acidity, bond energy, and electron affinity estimates, an isodesmic reaction approach was employed, wherein the acidities and bond energies were calculated relative to methane, and the electron affinities were calculated relative to methyl radical. Absolute values were then derived by combining the computed differences with the accurately known experimental values:²⁶ $\Delta H_{\text{acid}}(\text{CH}_4) = 416.7$ kcal/mol, $DH_{298}[\text{CH}_3\text{–H}] = 104.9$ kcal/mol, and $\text{EA}(\cdot\text{CH}_3) = 1.8$ kcal/mol. For comparison, the directly calculated acidity and bond enthalpy for methane and electron affinity for methyl radical obtained from G2(MP2) and CBS-4 methods are (in kcal/mol) 418.2, 105.7, and 0.97 (G2(MP2), and 419.4, 105.7, and 1.5 (CBS-4).

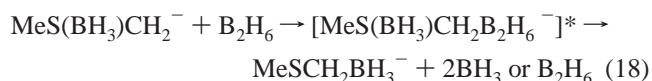
Discussion

The observed differences in the reactivity of **1a** and the authentic borate ions **1b,c** clearly indicate that deprotonation of complex **1** produces a stable carbanion that does not rearrange

to either of the lower energy forms under thermal conditions at room temperature. The model calculations indicate a high barrier for the exothermic [1,2]-BH₃ shift from sulfur to carbon, 29.3 kcal/mol (Figure 4), in keeping with the orbital symmetry-forbidden nature of such a process occurring with retention at boron.⁴⁹ Isomerization of **1a** to **1b** resembles the sulfonium ylide–sulfide rearrangement, in which an alkyl group migrates from sulfur to the ylide carbon. This rearrangement also has a relatively high barrier and is believed to proceed via radical pair intermediates.⁵⁰ The occurrence of carbanion reactivity, i.e., H/D exchange and electrophilic additions, by ions **2a**, **3a**, and **4a** also indicate formation of stable carbanions by deprotonation of the corresponding neutral borane complexes. Analogous orbital symmetry constraints on the unimolecular isomerization of these species are likely.

Isomerization of **1a** to **1c** has a 27.6 kcal/mol barrier and proceeds via a Wittig-like [1,2]-CH₃ anion shift mechanism analogous to that for the uncomplexed CH₃SCH₂⁻ carbanion.^{50,54} This rearrangement can be induced by collisional activation and is probably responsible for the anomalously low CID threshold energy obtained for BH₃ cleavage from ion **1a**, i.e., the dissociation product at threshold is CH₃CH₂S⁻ rather than CH₃SCH₂⁻.

The remote possibility exists that a mixture of **1a**, **1b**, and/or **1c** ions is formed in the flow tube, since the latter two isomers were unreactive and, thus, could have gone undetected by the probe reactions. Although isomerization of **1a** to either **1b** or **1c** by unimolecular processes at room temperature is unlikely, we must consider possible bimolecular pathways for converting **1a** to **1b**. The occurrence of the borane switching reaction illustrated in eq 5b raises the question as to whether **1a** can undergo isomerization to **1b** in the presence of the neutral diborane that is unavoidably present in the flow tube when sampling the head vapors from **1**. Equation 18 illustrates a



plausible mechanism for this, wherein ion **1a** first coordinates with B₂H₆ by B–C bond formation, followed by cleavage of the S–B bond to effect the overall isomerization. The thermodynamic viability of this reaction is determined by the fate of the two BH₃ product molecules: the reaction is predicted by ab initio calculations (G2(MP2)) to be endothermic by 9.8 kcal/mol if two separate BH₃ molecules are produced, but exothermic by 27.6 kcal/mol if they wind up bonded together as B₂H₆. In the latter case, B₂H₆ is a catalyst for the isomerization. While considered unlikely,⁵⁵ this possibility for formation of a mixture of **1a,b** by the latter process under the conditions of our experiments cannot be completely ruled out.

(51) Eisenstein, O.; Kayser, M.; Roy, M.; McMahon, T. B. *Can. J. Chem.* **1985**, *63*, 281.

(52) Sakai, S. *J. Phys. Chem.* **1995**, *99*, 9080.

(53) DiMare, M. *J. Org. Chem.* **1996**, *61*, 8378.

(54) Ahmad, M. R.; Dahlke, G. D.; Kass, S. R. *J. Am. Chem. Soc.* **1996**, *118*, 1398 and references therein.

These same considerations pertain to formation of borate isomer contaminants with ions **2a–3a**.

The results reveal that coordination of Me₂S, Me₃N, and Me₃P by BH₃ increases the gas-phase acidities of the methyl groups by 18–20 kcal/mol. The G2(MP2) and CBS-4 models predict absolute acidities for **1–3** that are in good agreement with experiment (Table 3). A larger increase in α -CH acidity (27 kcal/mol) is predicted by the CBS-4 calculations to accompany BF₃ coordination of Me₂S. Bracketing experiments with **4** and **4a** give a lower limit for the enhancement of 22 kcal/mol.

The origin of the acidity increases is the presence of the large bond dipole in the Lewis acid–base complexes, i.e., differential intramolecular electrostatic (inductive and field) effects on the conjugate acid–base pairs. The calculated geometry changes and charge distributions accompanying deprotonation of **1** (and **4**) clearly show this (Figure 2, Table 1). A significant reduction in the S–CH₂[−] bond distance accompanies deprotonation. Examination of the computed geometries for **2**, **3**, and their conjugate base anions shows the same thing. Resonance stabilization through S_{d π} –C_{p π} conjugation is not the explanation. Numerous experimental and theoretical studies show that the high-lying, virtual d-orbitals of main-group elements such as S and P do not participate in π -bonding to carbon or other first-row elements.⁵⁶ The negligible computed charge shifts to the heteroatoms that accompany deprotonation (Table 1) and the fact that the CH₂[−] groups in carbanions **1a–4a** remain strongly pyramidalized are inconsistent with d π –p π conjugation. Moreover, conjugation of this type is not possible with **2a**, but the measured acidity enhancement and the computed geometry changes in the ion are the same as in **1a** and **3a**. Rather, the bond length decreases accompanying deprotonation are a result of the strong attractive electrostatic interaction between the negatively charged CH₂[−] groups and the positively charged, onium-like heteroatoms in the ions.

The gas-phase acidity of **1** is virtually identical to that of the isoelectronic molecule, dimethyl sulfoxide, and the acidities of **2** and **3** are comparable to the acidities computed for the corresponding *N*-oxide and *P*-oxide molecules (Table 4). The origins of the α -CH acidity enhancements accompanying oxidation and borane coordination of the heteroatom are believed to be the same. The nature of the acidity increase in going from Me₂S to DMSO has been a subject of interest for many years, and several explanations have been proposed, including S_{d π} –C_{p π} conjugation,⁵⁷ negative hyperconjugation^{45b,58} and intramolecular electrostatic effects.^{45,56b} The latter two explanations are the correct ones, in our view. Ion **1a** constitutes a dipole-stabilized carbanion⁵⁹ in which the large local dipole provided by the S⁺–BH₃[−] bond exerts the same type of Coulombic stabilization of the negative charge localized at the CH₂[−] group as does the S⁺–O[−] bond dipole in deprotonated DMSO. We note the additional qualification proposed by Streitwieser and co-workers^{45a} that the net affect in DMSO also includes a significant term from electrostatic destabilization of the neutral acid, in addition to stabilization of the conjugate base anion.

(55) Assuming comparable CID cross sections, the relative intensities of the CID fragment ions that are common to both **1a** and **1b** suggest that the amount of **1b** formed with **1a** cannot be significant, <3%.

(56) (a) Gilheany, D. G. *Chem. Rev.* **1994**, *94*, 1339. (b) Boche, G.; Lohrenz, J. C. W.; Cioslowski, J.; Koch, W. In *The Chemistry of Sulphur-Containing Functional Groups*; Patai, S., Rappaport, Z., Eds.; Wiley: New York, 1993; Chapter 7. (c) Dobado, J. A.; Martínez-García, M.; Molina, J. M.; Sundberg, M. R. *J. Am. Chem. Soc.* **1998**, *120*, 8461.

(57) (a) Wolfe, S.; Lajohn, L. A.; Bernardi, F.; Mangani, A.; Tonachini. *Tetrahedron Lett.* **1983**, *24*, 3789. (b) Wolfe, S.; Stolow, A.; Lajohn, L. A. *Tetrahedron Lett.* **1983**, *24*, 4071.

(58) Wolfe, S. In *Organic Sulfur Chemistry*; Bernardi, F., Csizmadia, I. G., Mangini, A., Eds.; Elsevier: New York, 1985; Chapter 3.

Additional insight regarding the nature of the acidity increases derives from the thermodynamic dissection of the acidities in terms of bond energy and electron affinity terms.²⁹ The experimental data summarized in Table 3 show that the main contributor to the 20 kcal/mol increase in acidity (decrease in ΔH_{acid}) of complex **1** compared to Me₂S is the increased electron affinity of MeS(BH₃)CH₂[•] radical (**1d**). That is, BH₃ coordination leads to a 18 kcal/mol increase in radical EA, but no significant change in the α -CH bond strength within the experimental errors. The theoretical predictions are consistent with the experimental results. According to the G2(MP2) model, the 21 kcal/mol computed acidity increase is composed of a 25 kcal/mol increase in EA, but only a 4 kcal/mol increase in BDE accompanying BH₃ coordination, while the CBS-4 model breaks down the 20 kcal/mol ΔH_{acid} increase into Δ EA and Δ BDE terms of 28 and 8 kcal/mol, respectively.⁶⁰ The computed thermochemical decompositions for complexes **2** and **3** show the same trend, i.e., the acidity enhancements are strongly dominated by the increased electron binding energies of the carbanions. The large differences between the Δ EA and Δ BDE contributions are interpreted as dipolar stabilization of the carbanions, rather than dipolar destabilization of the neutral radicals or the conjugate acids, since if the latter were true, the Δ BDE term would be comparable to, or even greater than, the Δ EA term.

Given the ion–dipole nature of the 20 kcal/mol increase in the acidity of **1**, it is instructive to compare its magnitude with the purely dipolar effect of a full positive charge on the acidity of the isoelectronic species trimethylsulfonium ion, Me₃S⁺. The gas-phase acidity of Me₃S⁺ (ΔH_{acid}) is calculated to be 253 kcal/mol at the CBS-4 level of theory (Table 4). This represents a 120 kcal/mol greater acidity than that of **1** and a 140 kcal/mol acidity increase relative to Me₂S. A comparable effect on acidity due to charge–charge interactions in the conjugate base was recently reported by Cooks and co-workers⁶¹ for betaine, Me₃N⁺CH₂CO₂H. The experimentally determined gas-phase acidity of the carboxylic acid group in this cation was found to exceed that of *N,N*-dimethylglycine by about 100 kcal/mol. In the simplest of models for the difference between the acidities of Me₃S⁺ and Me₂SBH₃, we note that the computed distance between the negatively charged BH₃[−] and CH₂[−] groups in ion **1a** is about 3 Å, which would correspond to a Coulomb repulsion energy of approximately 112 kcal/mol for unit negative charges and unit dielectric constant.

The acidity enhancements that accompany borane coordination of Me₂S, Me₃N, and Me₃P in the gas phase are likely to be significantly attenuated in solution due to differential solvation of the complexed vs uncomplexed ions and neutral acids. Ignoring obviously important issues such as the nature of the counterion and differential ion-pairing effects for the moment, one would expect the *difference* in solvation free energies of the uncomplexed species (i.e., Me₂S and MeSCH₂[−]) to be greater than the *difference* in solvation free energies of the complexed species (i.e., **1** and **1a**), mainly due to the smaller intermolecular ion–solvent electrostatic term for **1a** compared to MeSCH₂[−]. This would translate directly into a reduction in

(59) Beak, P.; Reitz, D. B. *Chem. Rev.* **1978**, *78*, 275.

(60) The difference between the computed balance of electron affinity and bond energy terms given by the two models suggests that CBS-4 exaggerates the instability of the borane-complexed radical. This probably arises from the low-level (HF/3-21G*) used by this method for the geometry optimizations.

(61) Patrick, J. S.; Yang, S. S.; Cooks, R. G. *J. Am. Chem. Soc.* **1996**, *118*, 231. A slightly higher value for the acidity of betaine was reported by Williams and co-workers: Price, W. D.; Jockusch, R. A.; Williams, E. R., *J. Am. Chem. Soc.* **1998**, *120*, 3474.

the acidity enhancements in taking the Lewis acid–base complexes from the gas phase to solution. Partial support for this expectation is obtained from the results of a simple solvent continuum (SCRF)⁶² calculation of the relative acidities of **1** and Me₂S. At the MP2(full)/6-31G(d,p) level, the computed 24.5 kcal/mol gas-phase acidity enhancement accompanying BH₃ coordination of Me₂S drops by 3.8–4.5 kcal/mol with inclusion of a solvent continuum in the calculation corresponding to dielectric constants of 10–80. More sophisticated treatments⁶³ such as Monte Carlo type simulations of the acidity and solvation energy changes for the compounds examined in the present study would be most instructive.

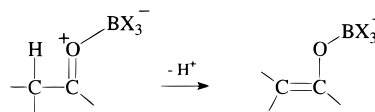
In addition to enhancing α -CH acidity, borane coordination increases the reactivity of the alkyl groups appended to the n-donor atom toward nucleophilic substitution and elimination. A thermodynamic explanation suffices. Coordination of a Lewis acid to an n-donor atom in a molecule necessarily decreases the heterolytic bond dissociation energies of attached alkyl groups, thereby facilitating their cleavage. For example, the S–C heterolytic bond energy of Me₂S (methyl cation affinity of MeS[−]) is 257 kcal/mol,²⁶ while G2(MP2) calculations give a S–C heterolytic bond energy for borane–dimethyl sulfide complex **1** (methyl cation affinity of MeSBH₃[−]) that is 26 kcal/mol smaller (231 kcal/mol). The difference results from the much stronger S–B bond in MeSBH₃[−] compared to that in Me₂SBH₃. Therefore, any nucleophilic displacement at a methyl group in **1** will be associated with a 26 kcal/mol larger enthalpy decrease compared to that for uncomplexed Me₂S. For instance, displacement of MeF from Me₂S by F[−] is near-thermoneutral ($\Delta H = -2$ kcal/mol²⁶) and is not observed, presumably due to a substantial energy barrier, while reaction 8 is strongly exothermic ($\Delta H = -28$ kcal/mol) and readily occurs under the conditions of our experiments. The same interpretation serves for β -eliminations: the endothermic eliminations of CH₂=CH₂ from Et₃N and Et₂O by NH₂[−] and F[−] are made exothermic and observable by borane coordination to the heteroatoms.

Conclusion

We have shown that coordination of simple n-donor molecules by BH₃ and BF₃ produces large changes in the gas-phase acidities and reactivity of the pendant alkyl groups. Deprotonation of the sulfide, amine, and phosphine complexes **1–4** produces stable α -carbanions that do not rearrange to the corresponding borate isomers. The acidity of the α -CH bonds in dimethyl sulfide, trimethylamine, and trimethylphosphine are increased by 18–20 kcal/mol by borane coordination to the

heteroatoms. A thermochemical decomposition of the acidity changes in terms of electron affinities and homolytic bond energies shows that large increases in the electron binding energies of the carbanions accompany borane coordination to the adjacent heteroatoms. This is due to electrostatic stabilization of the negatively charged CH₂[−] group in the ions by the dipolar Lewis acid–base bond. Ab initio theoretical models are in good accord with the experimental results, and they provide a detailed picture of the electrostatic interactions leading to the acidity enhancements. The kinetic stability of the dipole-stabilized carbanion **1a** with respect to isomerization to either of the more stable borate ion isomers **1b** or **1c** is shown by the calculations to be due to relatively high barriers (28–29 kcal/mol) for both [1,2]-BH₃ and [1,2]-CH₃ shifts. In addition to increasing α -CH acidity, borane coordination also labilizes the heteroatom–alkyl bonds in alkyl sulfides, amines, phosphines, and ethers. This leads to enhanced reactivity of the alkyl groups toward nucleophilic attack and β -elimination reactions.

In the Introduction, we began by citing the aldol condensation as an example of a familiar reaction in which Lewis acid catalysts must be exerting a large influence on the acidities of the substrates, in this case aldehydes and ketones. It is readily predicted that the acidity changes attending borane complexation of an aldehyde or ketone will be even greater than the already large effects on n-donor alkyls demonstrated in this work. This is because deprotonation of an aldehyde–borane complex will result in substantial intramolecular charge transfer to form a borate ion with a significantly stronger B–O bond, while for the n-donor alkyl complexes, the carbanion stabilization arises from weaker intramolecular ion–dipole interactions:



Measurements of the gas-phase acidities of borane complexes of simple aldehydes and ketones are currently in progress in our laboratory that confirm this expectation.⁶⁴ The preliminary results indicate acidity enhancements for borane–aldehyde complexes that are more than twice as large as those measured for the borane complexes examined in the present study.

Acknowledgment. This work was supported by the National Science Foundation.

Supporting Information Available: Listings of selected optimized geometries and total energies (in GAUSSIAN archive format) for borane and trifluoroborane complexes and related molecules (10 pages, print/PDF). See any current masthead page for ordering information and Web access instructions.

JA9804518

(64) Ren, J.; Squires, R. R. Manuscript in preparation.

(62) Wong, M. W.; Wiberg, K. B.; Frisch, M. J. *J. Chem. Phys.* **1991**, *95*, 8991.

(63) (a) Jorgensen, W. L.; Briggs, J. M. *J. Am. Chem. Soc.* **1989**, *111*, 4190. (b) Evaseck, J. D.; Houk, K. N.; Briggs, J. M.; Jorgensen, W. L. *J. Am. Chem. Soc.* **1994**, *116*, 10630.